Response of Retinal Blood Flow to Systemic Hyperoxia as Measured with Dual-Beam Bidirectional Doppler Fourier-Domain Optical Coherence Tomography

René M. Werkmeister[1], Stefan Palkovits[2], Reinhard Told[1,2], Martin Gröschl[3], Rainer A. Leitgeb[1], Gerhard Garhöfer[2], Leopold Schmetterer[1,2]*

1 Center for Medical Physics and Biomedical Engineering, Medical University of Vienna, Vienna, Austria, 2 Department of Clinical Pharmacology, Medical University of Vienna, Vienna, Austria, 3 Institute of Applied Physics, Vienna University of Technology, Vienna, Austria

Abstract

Purpose: There is a long-standing interest in the study of retinal blood flow in humans. In the recent years techniques have been established to measure retinal perfusion based on optical coherence tomography (OCT). In the present study we used a technique called dual-beam bidirectional Doppler Fourier-domain optical coherence tomography (FD-OCT) to characterize the effects of 100% oxygen breathing on retinal blood flow. These data were compared to data obtained with a laser Doppler velocimeter (LDV).

Methods: 10 healthy subjects were studied on 2 study days. On one study day the effect of 100% oxygen breathing on retinal blood velocities was studied using dual-beam bidirectional Doppler FD-OCT. On the second study day the effect of 100% oxygen breathing on retinal blood velocities was assessed by laser Doppler velocimetry (LDV). Retinal vessel diameters were measured on both study days using a commercially available Dynamic Vessel Analyzer. Retinal blood flow was calculated based on retinal vessel diameters and red blood cell velocity.

Results: As expected, breathing of pure oxygen induced a pronounced reduction in retinal vessel diameters, retinal blood velocities and retinal blood flow on both study days ($p < 0.001$). Blood velocity data correlated well between the two methods applied under both baseline as well as under hyperoxic conditions ($r = 0.98$ and $r = 0.75$, respectively). Data as obtained with OCT were, however, slightly higher.

Conclusion: A good correlation was found between red blood cell velocity as measured with dual-beam bidirectional Doppler FD-OCT and red blood cell velocity assessed by the laser Doppler method. Dual-beam bidirectional Doppler FD-OCT is a promising approach for studying retinal blood velocities in vivo.

Introduction

Ocular perfusion abnormalities are common and seen in a wide variety of diseases including glaucoma, diabetic retinopathy and age-related macular degeneration [1,2,3]. Nevertheless no gold standard method is available for quantifying blood flow in clinical use. Ultrasound color Doppler imaging is widely used for clinical studies, but information is limited to retrobulbar blood velocities and quantification of blood flow is hampered by the lack of diameter data [4]. Laser Doppler flowmetry and laser Speckle techniques can be used to assess optic nerve head and choroidal blood flow, but can provide only relative values of flow data [5,6]. Retinal vessel diameters can be quantified using fundus cameras, but this technique provides no information on blood velocity [7]. Combined with fundus photography Laser Doppler Velocimetry (LDV) enables measurement of absolute blood flow in individual retinal vessels [8,9,10,11]. By measuring all vessels entering the optic nerve head total retinal flow can be determined [10,12], but long acquisition times and high patients' compliance are required.

Approximately 15 years ago first attempts were made to extract velocities by using optical coherence tomography (OCT) initially based on time domain OCT (TD-OCT) [13,14]. Later approaches included variation of the coherence length [15] before phase sensitive detection allowed for extraction of velocities based on Fourier domain OCT (FD-OCT) [16,17]. Several approaches were introduced in order to overcome the problem of the unknown Doppler angle, i.e. the angle between the incident probe beam and the vessel under study. This angle is required for measurement of absolute velocities, e.g. illumination of the sample with multiple probe beams [18,19], extraction of the Doppler angle from multiple B-scans [20,21] or extraction of the Doppler

angle from a 3D volume [22,23]. In order to overcome the problem in determining the angle between incident light and the vessel orientation, we introduced a dual-beam bidirectional Doppler FD-OCT system allowing for extraction of absolute blood velocity independently of the Doppler angle [24]. In the present study we investigated the response of retinal blood flow to 100% oxygen breathing using this system and compared the data with those obtained from a bidirectional LDV system.

Methods

Ethics Statement

The study protocol entitled "The validity of retinal blood flow measurement during hyperoxia in humans using Fourier domain CDOCT" was approved by the Ethics Committee of the Medical University of Vienna.

A total of 10 healthy subjects aged between 19 and 35 years participated in this study. The nature of the study was explained to all subjects and they gave written consent to participate. An ophthalmic examination, including slit lamp biomicroscopy and indirect funduscopy, was performed. Inclusion criteria were normal ophthalmic findings and ametropia of less than 1 diopter. In addition, a physical examination was done including electro cardiogram (ECG) and measurement of blood pressure (Infinity Delta, Dräger Medical Austria GmbH, Vienna, Austria) and pulse rate. Subjects were excluded if any abnormality was evident.

Two study days were scheduled for each subject. Both study days followed an identical schedule, but on one study day retinal blood velocities were measured using bidirectional LDV and on the other study day using dual-beam bidirectional Doppler FD-OCT. The sequence of the study days was randomized. For measurements in healthy volunteers pupils were dilated with one drop of tropicamide ("Mydriaticum Agepha®-eyedrops, 5 mg/ml tropicamide, AGEPHA GmbH, Vienna, Austria). During the study days a resting period of at least 20 minutes in a sitting position was scheduled to allow for stabilization of blood pressure and pulse rate. Thereafter, baseline measurement of retinal vessel diameter of a major temporal vein was done using the Dynamic Vessel Analyzer (DVA). This was followed by baseline measurements of retinal blood velocities at the same position where the diameter assessment took place with either LDV or dual-beam bidirectional Doppler FD-OCT, respectively, on both study days. Then a period of 100% oxygen breathing was scheduled and 15 minutes after the start of oxygen breathing retinal vessel diameters and retinal blood velocities were measured again. This time regimen was used because we have previously shown that the vasoconstrictor response to hyperoxia stabilizes after approximately 6 minutes [25]. On the second study day, the subjects crossed over to the other measuring device for retinal blood velocity. Dynamic vessel analyzer was also used on the second study day for the evaluation of vessel diameter. Oxygen (100%) (gases for human use, Messer; Vienna, Austria) was delivered through a partially expanded reservoir bag at atmospheric pressure. For gas delivery a face mask which covered mouth and nose connected to a two-valve system, preventing the subject from rebreathing was used. Intraocular pressure was measured after completion of blood flow assessment using applanation tonometry, blood pressure was measured non-invasively on the upper arm, and pulse rate was measured using a pulse oximeter (Infinity Delta, Dräger Medical Austria GmbH, Vienna, Austria).

Dual-beam bidirectional Doppler FD-OCT

The setup of the dual beam bidirectional Doppler FD-OCT was described previously [24]. The basic principle of the instrument is to illuminate the vessel with two probe beams characterized by the wave vectors $\vec{K}_1$ and $\vec{K}_2$. The beams are separated by their polarization properties and impinge onto the sample given by the velocity vector $\vec{v}$ from two distinct directions. With this illumination and detection scheme, the measurement becomes independent of the exact angle of incidence of the probe beams. The phase shifts $\Phi'_{1,2}$, caused by the scattering of the impinging light at the red blood cells are given by $\Phi'_i = 2\vec{K}_i\vec{v}_i\tau$ $(i=1,2)$ for the two beams, respectively. In this equation $\vec{v}_i$ are the velocity vectors of the moving red blood cells (RBC) pointing in the direction of the corresponding probe beams i. τ is the time span between two subsequent recordings, equaling the exposure time of the camera. The light backscattered from each probing channel is collected by two identical spectrometers, where the spectral modulations are detected as a function of frequency and the depth profile is calculated from an inverse Fast Fourier Transform $(FFT)^{-1}$.

Using simple trigonometry it can be shown that

$$V_{abs} = \Delta\Phi \frac{\lambda}{4\pi \cdot n \cdot \tau \cdot \Delta\alpha \cdot \cos\beta} \qquad (1)$$

where $\Delta\Phi = \Phi_1 - \Phi_2$. Φ_i are the post-processed phase shifts, λ is the central wavelength of the light source, β is the angle of the velocity vector with respect to the detection plane, $\Delta\alpha$ is the separation angle of the two beams at the retina and n is the group refractive index of blood, which was estimated as 1.37 [26]. With a parallel displacement of the two probe beams of 2 mm, the separation angle $\Delta\alpha$ at the ocular fundus for a standard eye length of 24.2 mm [27] is 4.7 degree. For determination of the angle β an additional scanning laser ophthalmoscope (SLO) detection arm measuring the back-reflected light is added to obtain an *en face* fundus image. This is achieved by placing the tangent to the vessel at the measured position and calculating the slope with simultaneous consideration of the true dimensions of the SLO image, i.e. $\beta = \tan^{-1}(w_{sl,x}/w_{sl,y})$ (Figure 1). Furthermore, the system comprises a custom built fundus camera that is coupled into the OCT sample arm by means of a dichroic mirror and allows for exact focal overlap of the two probe beams and inspection of the ocular fundus during the whole measurement time.

The system operates at a center wavelength λ of 839 nm with a bandwidth $\Delta\lambda$ of approximately 52 nm, resulting in an axial resolution in air of 6 µm. The time period between two subsequent CCD recordings (A-scans) is 56 µs, resulting in a frame rate of $9s^{-1}$ with a lateral tomogram dimension of 2000 A-lines. The maximum velocity that can be measured in the regions of the optic nerve head without any wrapping artifacts is approximately 20 mm/s. When phase wrapping in the center of the vessels is corrected as outlined in detail below, the maximum detectable velocity can almost be doubled. The oversampling factors (OF) of the phase tomograms – defined as $OF = w \cdot N/d$ [28], where w is the spot size, N is the number of sampling points and d the geometric width of the tomograms–is 21 in our case. The power of both probe beams incident on the cornea was measured with 650 µW, which is below the ANSI (American National Standard Institute) limits for small source ocular exposure to a laser beam within the measuring time [29].

Even though the acquisition of a single tomogram in vivo takes only about a tenth of a second, any movement of the eye relative to the laser beam is a problem in phase-sensitive Doppler OCT, because it induces a phase-shift unrelated to blood flow. Therefore, the phase tomograms need to be corrected for those sample movements. For this purpose, the histogram-based
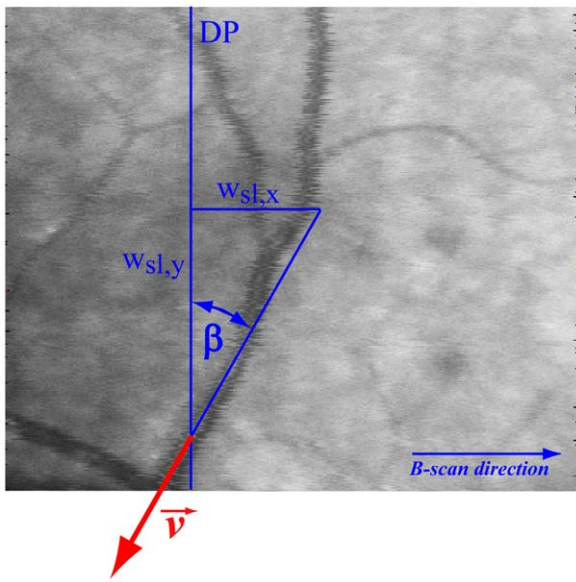
Figure 1. SLO fundus image of a venous junction. Angle β is determined from the slope of the tangent to the vessel at the measured location. $w_{sl,x}$, $w_{sl,y}$; image width in x- and y-direction. DP; detection plane.

doi:10.1371/journal.pone.0045876.g001

approaches presented by Makita et al. [30] and Schmoll et al. [31] were optimized for movement correction in presence of large vessels. The modified algorithm uses the histogram not only for detection of the phase offset due to background motion, but also to distinguish between A-scans containing tissue only and A-scans containing both tissue and vessels.

After bulk motion correction the vessel position in the phase image is detected by convolution of the image with an elliptic template. The size of the template is set according to the dimensions of the selected vessel in the tomogram. The phase shift Φ'_i between adjacent A-scans is calculated as $\Phi'(z) = \arg\left[I^*_{n+1}(z) \cdot I_n(z)\right]$, where z is the axial position, $I_n(z)$ is the complex signal calculated by the inverse FFT of the nth scan, and I^* is the complex conjugate. Thus, the values for Φ'_i are in the range $[-\pi, \pi]$. However, especially in arteries and large veins the velocity values can exceed the unambiguous velocity range leading to phase wrapping artifacts, i.e. a reversal of the measured flow direction in the center of the vessel. Such phase wraps can easily be corrected by determining the flow direction based on the phase shift values close to the vessel walls. As such, the phases in the center of the vessel are mapped into the range $[0,2\pi]$ by $\Delta\Phi = \Delta\vartheta + 2\pi$ (if $0 < \Phi_i \leq \pi$) or into the range $[-2\pi, 0]$ by $\Delta\Phi = \Delta\vartheta - 2\pi$ (if $-\pi \leq \Phi_i < 0$). Double phase wraps did not occur in any of the measured veins in the present study. Another problem relates to fringe washout occurring particularly at high flow velocities. The missing Doppler data are reconstructed by applying a parabolic fit to the available data points [22]. It has been previously shown that the blood velocity profile differs from parabolic in retinal vessels [32]. However, since only missing data points are reconstructed while the original data stay untouched, the error introduced by this assumption is expected to be small.

For calculation of the average phase within the vessel cross section area, the approach introduced by Szkulmowska et al. was used [33]. Briefly, the method takes into account that the phase shifts Φ' are randomly distributed around the actual value. Hence, when phase averaging is performed in the angular domain, the mean phase difference is underestimated particularly at high velocities. Therefore, the phase values are transformed to complex representation and the averaging is performed by calculating the argument of the complex sum. The average phase shift $\Phi_{1,2}$ within a certain vessel is calculated for each frame of a series of $100-120$ tomograms and for each detection channel separately. Afterwards, the actual phase difference $\Delta\Phi$ between the two probing channels is calculated by the simple subtraction $\Delta\Phi = \Phi_1 - \Phi_2$. A diagram explaining the steps involved in signal analysis in shown in Figure 2.

Laser Doppler Velocimetry and Dynamic Vessel Analyzer

For comparison, measurements were also done with a commercially available bidirectional laser Doppler velocimetry (LDV) system (LDV-5000, Oculix Inc., Arbaz, Switzerland) [9]. The principle of LDV is based on the optical Doppler effect. Laser light of a single-mode laser diode with a wavelength of 670 nm is scattered and reflected by moving erythrocytes leading to a broadened and shifted frequency spectrum. The frequency shift is proportional to the blood flow velocity in the retinal vessel. The maximum Doppler shift corresponds to the centerline erythrocyte velocity. The Doppler shift power spectra are recorded simultaneously for two directions of the scattered light. The scattered light is detected in the image plane of the fundus camera. This scattering plane can be rotated and adjusted in alignment with the direction of the velocity vector, which enables absolute velocity measurements. Blood flow values as well as velocity values were compared among LDV and Doppler OCT measurements.

In all these experiments retinal vessel diameters were measured in mydriasis with the Dynamic Vessel Analyzer (DVA, IMEDOS GmbH, Jena, Germany). This system comprises a fundus camera (FF 450, Carl Zeiss Meditec AG, Jena, Germany), a high-resolution digital video camera and a personal computer with analyzing software. For the determination of retinal vessel diameters, recorded images are digitized and analyzed in real-time with a frequency of 50 Hz. The system provides excellent reproducibility and sensitivity [7,34]. After selection of the measurement location, the DVA is able to follow the vessels during movements within the measurement window.

Effect of eye movements

The geometrical situation at the posterior pole of the eye is depicted in Figure 3(a). Here α_1 and α_2 are two angles of the beams impinging on the retinal blood vessels, i.e. the Doppler angles, and $\Delta\alpha$ is the difference between these angles as mentioned above. γ is the angle between the plane perpendicular to the optical axis of the illuminating beam and the velocity vector $\vec{v}$, and β is the angle between the plane spanned by $\vec{K}_1$ and $\vec{K}_2$ and the velocity vector $\vec{v}$. The phase shifts in the two channels can then be expressed as

$$\Phi_1 = V \cdot \frac{4\pi n \tau \cos\beta}{\lambda} \cdot \sin\left(\frac{\pi}{2} - \alpha_1 - \gamma\right) \qquad (2)$$

$$\Phi_2 = V \cdot \frac{4\pi n \tau \cos\beta}{\lambda} \cdot \sin\left(\frac{\pi}{2} - \alpha_2 - \gamma\right)$$

Assuming an emmetropic eye in which $\Delta\alpha$ is 4.7 degrees or 0.082 rad, defining ε as $\alpha_1 - \gamma$ and considering that *in vivo* $(\pi/2 - \varepsilon)$ is very small, Equation 2 can be re-written as

$$\Phi_1 = V \cdot \frac{4\pi n \tau \cos\beta}{\lambda} \cdot \left(\frac{\pi}{2} - \varepsilon\right) \qquad (3)$$
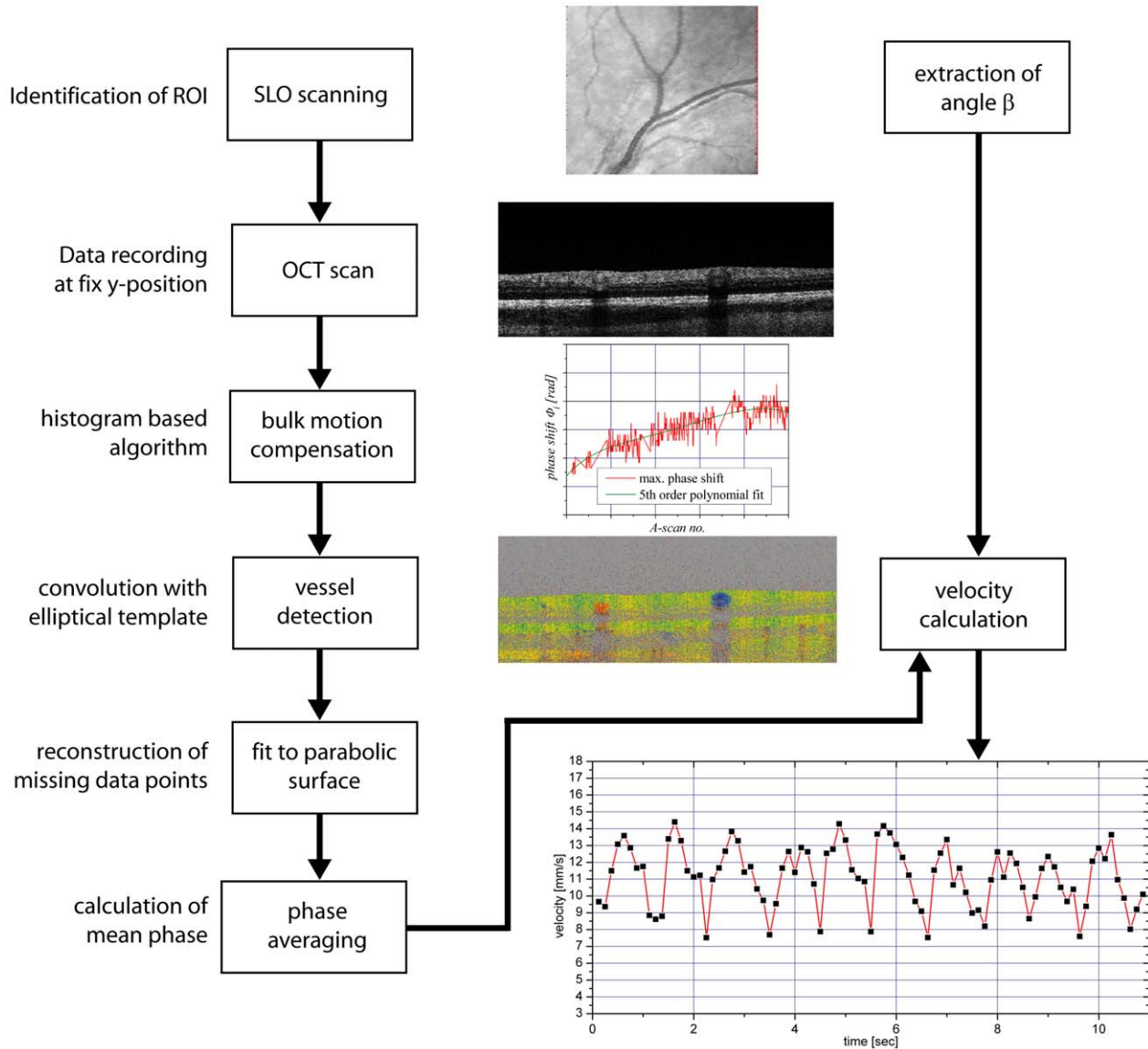
Figure 2. Flow chart for bidirectional Doppler FD-OCT. Flow chart explaining velocity extraction based on bidirectional Doppler FD-OCT.
doi:10.1371/journal.pone.0045876.g002

$$\Phi_2 = V \cdot \frac{4\pi n\tau \cos\beta}{\lambda} \cdot \left(\frac{\pi}{2} - \varepsilon - 0.082\right)$$

by replacing $\sin(\pi/2 - \varepsilon)$ by the angle itself. As mentioned above, the difference in the phase is used to calculate the absolute velocity within the vessel (equation 1). Once absolute velocity is calculated, the angle ε can be extracted based on equation 3. Since this can be done independently for both channels, the results of these calculations can serve as a proof for the validity of the dual beam bidirectional concept in the *in vivo* situation.

Assuming that the eye slightly moves during measurement and that accordingly γ is changed into $\gamma + \Delta$ (red coordinate system in Figure 3(b)) and that the velocity changed from a value V_1 into a value $V_2 = k \cdot V_1$. The phase shifts in the two channels then change to

$$\Phi_1^{\delta,V} = k \cdot \left(\Phi_1 + \Delta \cdot \frac{4\pi n\tau \cos\beta}{\lambda}\right) \quad (4)$$

$$\Phi_2^{\delta,V} = k \cdot \left(\Phi_2 + \Delta \cdot \frac{4\pi n\tau \cos\beta}{\lambda}\right).$$

As such, while measuring the phase from each of these channels, it is unclear whether an observed change in phase is due to a change in blood velocity or a change in the angle of incidence. In the case that $\Delta = 0$ under optimal conditions, Φ_1^V becomes $k \cdot \Phi_1$ and Φ_2^V becomes $k \cdot \Phi_2$. In this case the change in velocity as expressed by a factor k, which is adequately mirrored in the data from both channels. If only Δ changes and V stays constant equation 4 simplifies to
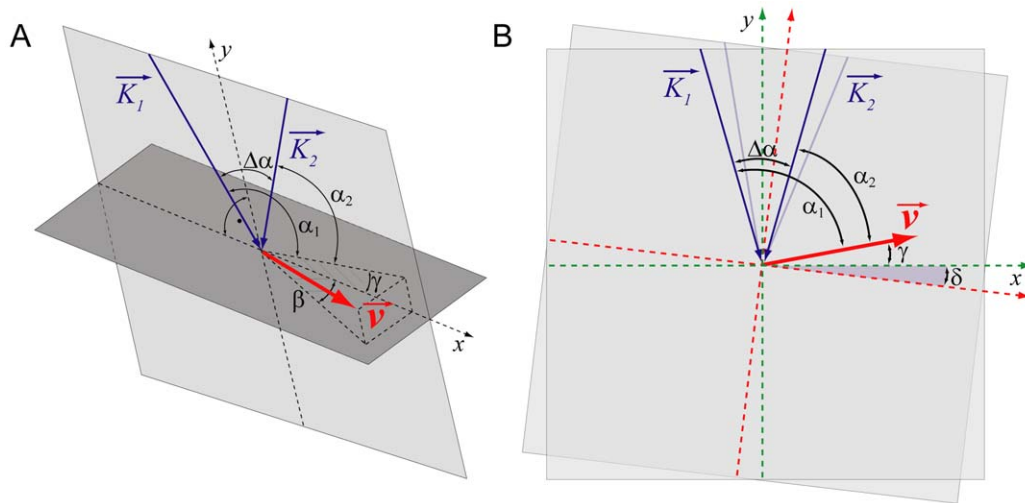
Figure 3. Geometrical situation at the posterior pole of the eye. $\vec{K}_1$ and $\vec{K}_2$, probe beam wave vectors; $\vec{v}$, velocity vector; α_1 and α_2, Doppler angles; $\Delta\alpha$, separation angle between probe beams; γ, angle between $\vec{v}$ and the plane perpendicular to the detection plane; δ, change in illumination angle due to eye movement.
doi:10.1371/journal.pone.0045876.g003

$$\Phi_1^\delta = \left(\Phi_1 + \Delta \cdot \frac{4\pi n \tau \cos\beta}{\lambda} \right) \qquad (5)$$

$$\Phi_2^\delta = \left(\Phi_2 + \Delta \cdot \frac{4\pi n \tau \cos\beta}{\lambda} \right).$$

Note that in this case a change in velocity would be assumed relying on information from one channel only. Even if Δ is very small; the effect on the phase might be huge depending on the absolute values of α_1 and α_2. Assuming that $\alpha_1 - \gamma$ is 92.35 degrees and $\alpha_2 - \gamma$ is 87.65 degrees a movement of only 1 degree ($\Delta = 1$ degree) would result in k-values of 1.43 and 0.57 for the data extracted from the two channels, respectively. The situation is even more severe in case the geometry is less symmetrical to the optical axis of the eye. If we assume that $\alpha_1 - \gamma$ is 94.12 degrees and $\alpha_2 - \gamma$ is 89.88 degrees a movement of $\Delta = 1$ degree would result in k-values of 2.46 and -0.75 for the data extracted from the 2 channels, respectively. This means that data from channel one would erroneously imply that velocity has more than doubled, whereas data from channel 2 would even imply that velocity changed its direction. This is the case although absolute blood velocity stayed constant and Δ changed by 1 degree only.

Changes in the angle β are much less critical. Assuming that β is 45 degrees, a change of β of 5 degrees only results in a k of 0.92 in both channels.

The same principle applies to bidirectional laser Doppler velocimetry, although the geometry is slightly different, because the eye is illuminated by one laser beam only, and the scattered laser light is detected in two distinct directions. Generally the frequency shift in the two channels is given by f_1 and f_2, respectively, and absolute velocity can be calculated as $\Delta f = f_1 - f_2$.

$$f_1 = V \cdot \frac{n\cos\beta}{\lambda} \cdot \left(\sin\left(\frac{\pi}{2} - \gamma - \alpha_1 \right) \right) \qquad (6)$$

$$f_2 = V \cdot \frac{n\cos\beta}{\lambda} \cdot \left(\sin\left(\frac{\pi}{2} - \gamma - \alpha_2 \right) \right)$$

As such, small eye movements (changes in Δ) during LDV measurements have essentially the same impact as in bidirectional Doppler OCT, if one observes the signal in one of the two probing channels only.

Data analysis

Velocity data as obtained with OCT technology are termed $V(OCT)$ and data obtained with LDV technology are termed $V(LDV)$. Generally, velocity values V as presented in this article represent average values V_{mean} over the cross section of the vessel. In OCT, these data can be calculated from the actual measurements. In LDV, only the maximum Doppler shift can be extracted and V_{mean} was calculated as $V_{max}/2$ assuming a parabolic velocity profile [12]. Data at baseline are termed V_{BL} and data during oxygen breathing are termed V_{O2}. The same nomenclature was used for diameter measurements resulting in values $d_{BL}(OCT)$, $d_{BL}(LDV)$, $d_{O2}(OCT)$ and $d_{O2}(LDV)$. All diameter measurements were done with the DVA. OCT and LDV in this case simply denotes that measurements were done on the OCT and LDV study days, respectively.

Oxygen reactivity was defined as $(1 - V_{O2}/V_{BL}) \cdot 100$. The same formula was used for diameter measurements. Total blood flow through the vein was calculated by $Q = V \cdot d^2 \cdot \pi/4$. The angle ε was extracted from equation 5 for the data obtained at both channels of the OCT system ($\varepsilon_1(OCT)$ and $\varepsilon_2(OCT)$). For this calculation small intervals of the phase shift time course were used, in which both phases showed only minor fluctuations. The same procedure was applied for the LDV system resulting in $\varepsilon_1(LDV)$ and $\varepsilon_2(LDV)$.

Statistical comparisons were done using repeated measures ANOVA and paired t-tests. In addition, Bland Altman graphs were prepared for comparison of data. A two-sided p-value of less than 0.05 was considered the level of significance.

Results

Table 1 summarizes the baseline data of the study population on the two study days. No difference was observed in blood pressure, pulse rate or vessel diameter. In addition, neither blood pressure nor pulse rate changed during 100% oxygen breathing (data not shown). Results of velocities, vessel diameters and blood flow during baseline and during 100% oxygen breathing are presented in Table 2 $V_{BL}(OCT)$ was slightly higher than $V_{BL}(LDV)$ (p = 0.01). A tendency towards higher velocity values with OCT was also seen during hyperoxia but the difference between the $V_{O2}(OCT)$ and $V_{O2}(LDV)$ did not reach the level of significance (p = 0.06). There was no difference in vessel diameters on the two study days during both baseline and hyperoxia conditions (baseline $d_{BL}(OCT)$ versus $d_{BL}(LDV)$ p = 0.86, hyperoxia $d_{O2}(OCT)$ versus $d_{O2}(LDV)$ p = 0.55). As expected from these results, blood flow $Q_{BL}(OCT)$ was also higher than $Q_{BL}(LDV)$ (p = 0.01). By contrast there was no significant difference between $Q_{O2}(OCT)$ and $Q_{O2}(LDV)$ although a tendency towards higher values was observed when OCT was employed (p = 0.09). The oxygen reactivity in velocity was comparable between the two study days (OCT day: 32.6±17.2%, LDV day: 35.8±15.7%, p = 0.44). The oxygen reactivity in blood flow was also comparable (OCT day: 51.7±13.2%, LDV day: 51.1±11.9%, p = 0.90) between the two applied method.

The correlation between $V_{BL}(OCT)$ and $V_{BL}(LDV)$ as well as $V_{O2}(OCT)$ and $V_{O2}(LDV)$ is presented in Figure 4. The degree of association was better during baseline conditions than during breathing 100% oxygen, although the correlation was highly significant under both conditions (p<0.01). The same applies to the correlation between $Q_{BL}(OCT)$ and $Q_{BL}(LDV)$ as well as $Q_{O2}(OCT)$ and $Q_{O2}(LDV)$ as shown in Figure 4. This is also reflected in the Bland Altman plots presented for V and Q in Figures 5 and 6, respectively. Generally, all values were slightly lower when measured with LDV as compared to OCT. The difference never exceeded 3 mm/s for velocity and 4 µl/min for blood flow measurements.

A sample measurement is presented in Figure 7. In both channels the reduction in velocity, but also the vasoconstriction in response to 100% oxygen breathing is clearly visible. The different colors indicate that in one channel the angle of incidence, i.e. the Doppler angle α, is below $\pi/2$, in the other channel above $\pi/2$. In channel 2 the angle is, however, obviously close to $\pi/2$.

Figure 8 and Figure 9 present phase extractions from two baseline measurements. In the example shown in Figure 8 the phases Φ_1 and Φ_2 were almost stable for the first 2 seconds. Thereafter, Φ_1 and Φ_2 showed a continuous change, which was, however, parallel for both channels. This is also seen from the

Table 1. Baseline blood pressure, pulse rate and vessel diameters at the two study days.

	Day 1	Day 2	p-value
Systolic blood pressure (mmHg)	118±9	117±9	0.80
Diastolic blood pressure (mmHg)	67±6	66±6	0.71
Pulse rate (beats/min)	64±9	63±7	0.78
Retinal vessel diameter (µm)	141.0±18.8	140.1±19.1	0.86

Table 2. Velocity, diameter and blood flow data under baseline conditions and during 100% oxygen breathing measured on Doppler OCT or Laser Doppler Velocimetry study day.

|	Baseline	O2	p-value
Velocity (OCT) [mm/s]	10.1±2.3	6.7±1.7	<0.001
Velocity (LDV) [mm/s]	9.2±2.3	5.9±1.9	<0.001
Diameter (OCT) [µm]	141±19	123±20	<0.001
Diameter (LDV) [µm]	140±19	122±17	<0.001
Blood flow (OCT) [µl/min]	10.3±2.9	5.0±2.2	<0.001
Blood flow (LDV) [µl/min]	9.0±2.7	4.2±1.8	<0.001

stability of $\Delta\Phi$ over time and as such represents a movement of the eye relative to the laser beams. Over time Φ_1 changed from −1.5 rad to 0.5 rad and Φ_2 changed from −0.75 rad to 1.25 rad. In the example shown in Figure 9, we also observed a drift in Φ_1 and Φ_2. In addition, several spikes in Φ_1 and Φ_2 were detected. A total of 7 spikes were observed during the measurement period. During all these spikes, which may reflect saccade-like eye movements, $\Delta\Phi$ remained constant.

Figure 10 shows the calculation of ε from Φ_1 and Φ_2 as presented in equation 3. Good agreement was found between the angles obtained at baseline in the OCT measurements (r = 0.999, p<0.001) and during 100% O_2 breathing (r = 0.999, p<0.001). The correlation between the angles before and during O_2 breathing was, however, weak and not significant (channel 1: r = 0.326, channel 2: r = 0.325). For LDV measurements, the correlation between the angles as calculated before (r = 0.855, p = 0.002) and during 100% O2 breathing (r = 0.937, p<0.001) was again significant, but the association was lower than in the OCT measurements. The correlations between the angles before and during O_2 breathing were significant, but only for channel 2 (channel 1: r = 0.373, channel 2: r = 0.690, p = 0.027).

Discussion

We present measurements of retinal blood flow velocity using bidirectional FD-OCT in healthy subjects during normoxia and hyperoxia and comparison with bidirectional LDV data. Generally, there is good agreement between the two techniques, but bidirectional FD-OCT offers several advantages that will be outlined in more detail below. Our data also indicate that single-beam techniques are extremely sensitive to movement artifacts. This makes it difficult to use them for measurement of absolute blood flow velocity, but also for quantifying changes in blood flow or blood flow velocity during stimulation.

Until the introduction of Doppler OCT, bidirectional LDV was the only technology capable of measuring absolute blood flow velocities in retinal vessels. Using this technique, absolute blood flow values in the retina have been published by several authors combing LDV with measurement of retinal vessel diameters. Riva and co-workers were the first to report measurements of total retinal blood flow with a value of 34±6 µl/min [10]. In subsequent publications, values between 37±5 µl/min and 80±12 µl/min were reported [11,12,35,36,37,38,39]. In the present study, good agreement was found between velocities as measured with LDV and OCT, although the values as obtained with the latter were slightly higher. Most likely, this is related to some methodological problems with the LDV system. Theoreti-
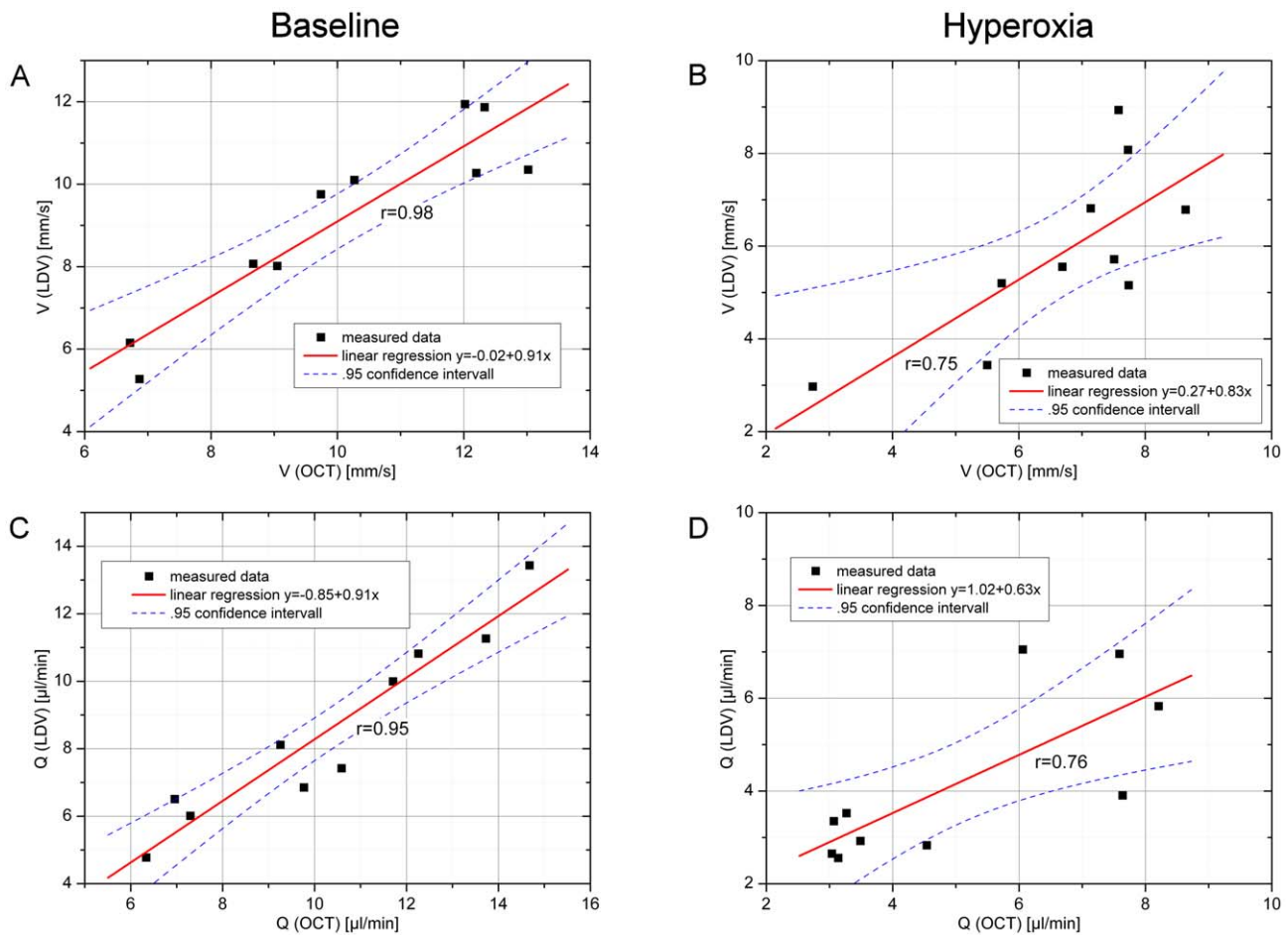
Figure 4. Correlation analysis for velocity measurements. Correlation between velocity and blood flow as assessed with LDV and OCT, respectively, during baseline conditions and during hyperoxia.
doi:10.1371/journal.pone.0045876.g004

cally, the power spectrum from a cylindrical tube with a flowing fluid is a rectangle, in which the center line velocity corresponds to the maximum of the frequency shift [8]. In reality, however, the power spectrum is non-rectangular and the validity of center line velocity extraction depends on the algorithm to estimate the maximum of the frequency shift [9]. Related to this problem is the
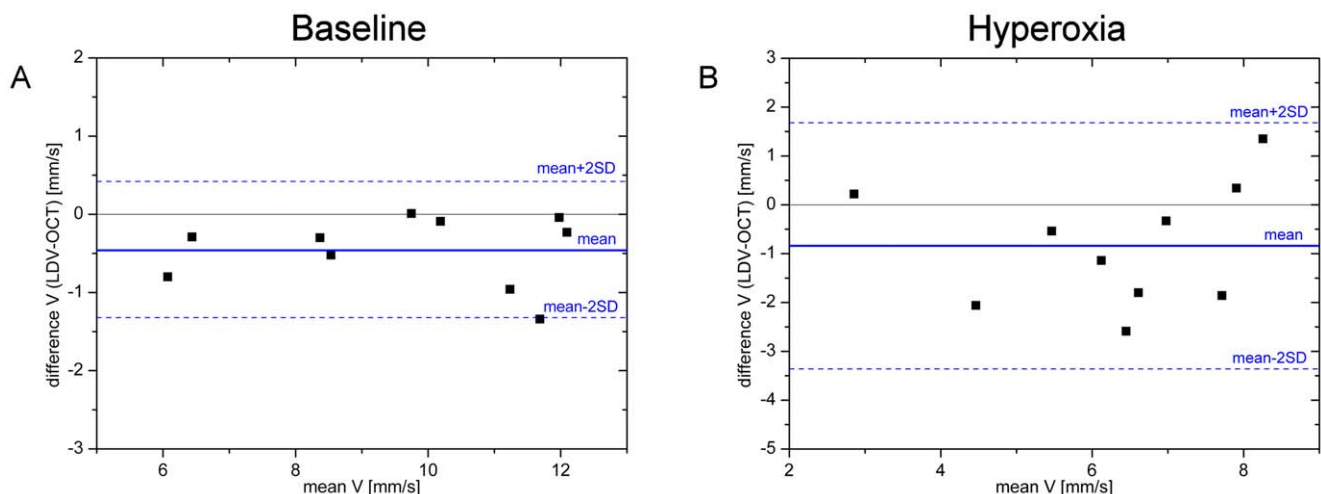
Figure 5. Bland-Altman of velocity measurements. Bland-Altman plot comparing velocity data as obtained with laser Doppler velocimetry and with bidirectional Doppler FD-OCT. Data are presented for baseline conditions as well as for conditions during systemic hyperoxia.
doi:10.1371/journal.pone.0045876.g005
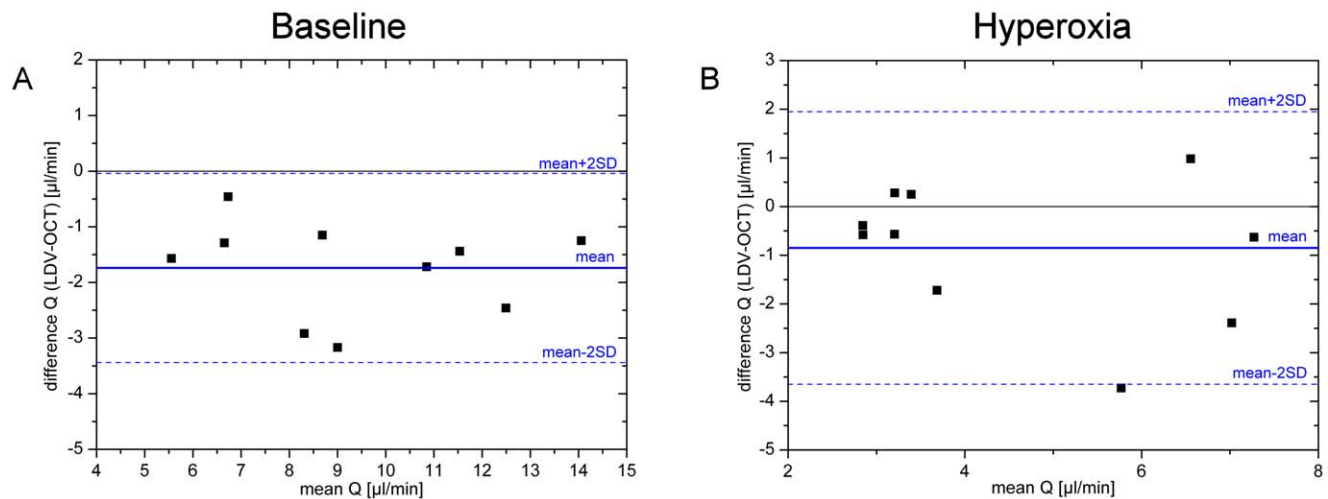
Figure 6. Bland-Altman plot of blood flow calculation. Bland-Altman plot comparing retinal blood flow data as calculated from measurements of blood flow velocity obtained either with laser Doppler velocimetry or with bidirectional Doppler FD-OCT combined with diameter measurements with the Dynamic Vessel Analyzer. Data are presented for baseline conditions as well as for conditions during systemic hyperoxia.
doi:10.1371/journal.pone.0045876.g006

question on how to calculate the mean velocity based on measurements of maximum velocity. Riva and co-workers in their original work used a factor of 1.6 based on in vitro measurements [10]. In vivo measurements using a scanning LDV, however, indicated very little deviation from a parabolic profile [40]. As such, we have used a factor of 2 in subsequent publications [35,41]. Recent work using an adaptive optics scanning laser ophthalmoscope, however, found much smaller values between 1.5 and 1.65 [32]. Using Doppler OCT, this assumption is less critical, because the actual velocity profile is measured. In our approach a theoretical assumption about the velocity profile is only required for reconstruction of missing data points.

Another problem with the Oculix LDV system is that during eye movements the laser beam may not hit the center of the vessel (unpublished observation). This may well lead to an underestimation of retinal blood flow velocities and most likely contributes to the lower velocity values as assessed with LDV. During states of vasoconstriction as induced by 100% oxygen breathing, this problem is obviously more severe. The Canon LDV system

overcomes this problem by using an eye tracker system allowing for automatic motion correction [42,43,44].

The absolute blood velocities as obtained in the present study as well as the effect of 100% oxygen breathing are in good agreement with previously published data. A variety of previous studies reported on the effect of 100% oxygen breathing on retinal blood flow and provided comparable data as those obtained in the present study [25,37,45,46,47]. This vasoconstrictor response is required to prevent the retinal tissue from toxic hyperoxia [48]. When comparing the data as obtained on the two study days, one needs to consider that neither the baseline diameter nor the hyperoxia-induced vasoconstriction was similar on the two study days. As such, the deviations from perfect association seen in Figures 4–6 may arise from two distinct phenomena, namely imperfections in the measurement procedures as discussed above and physiological day-to-day variability.

The present data clearly indicate that bidirectional Doppler OCT measurements are insensitive to changes in the angle of incidence of the laser beam on the vessel. This is evident from our
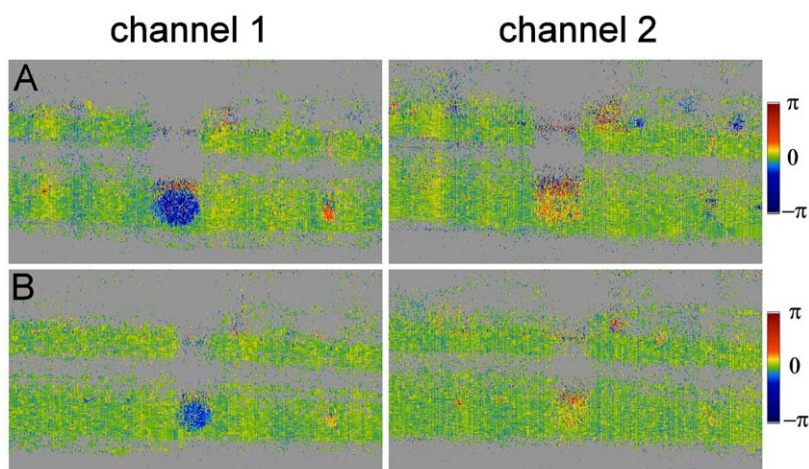
Figure 7. Phase tomograms at baseline and during hyperoxia. Sample OCT measurements as obtained in both channels during baseline conditions (A) and during breathing 100% oxygen (B). Vasoconstriction and reduction of velocity can be observed in the lower tomograms.
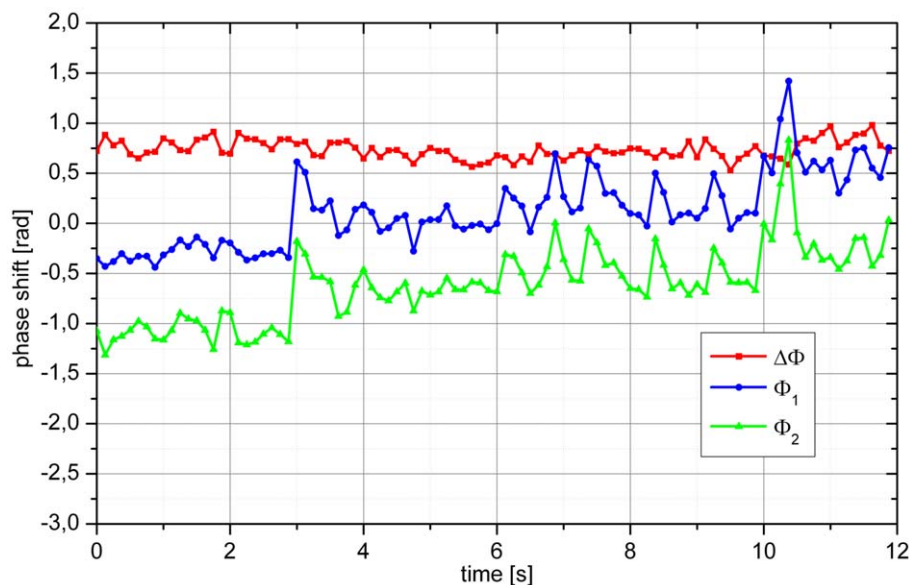doi:10.1371/journal.pone.0045876.g007
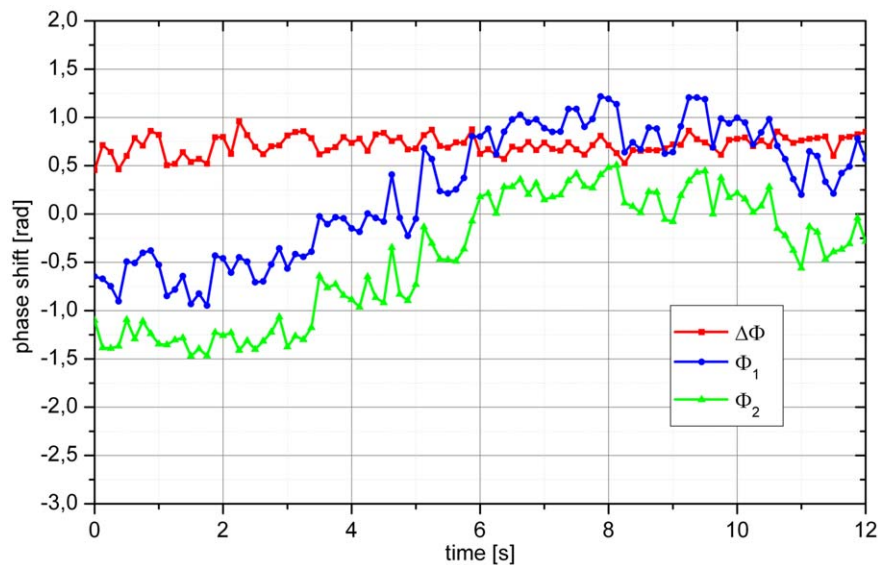
Figure 8. Sample phase extraction of a baseline measurement. Over the measurement period of 12 s the eye moved relative to the incoming laser beams resulting in pronounced changes in Φ_1 and Φ_2, but almost unchanged $\Delta\Phi$.
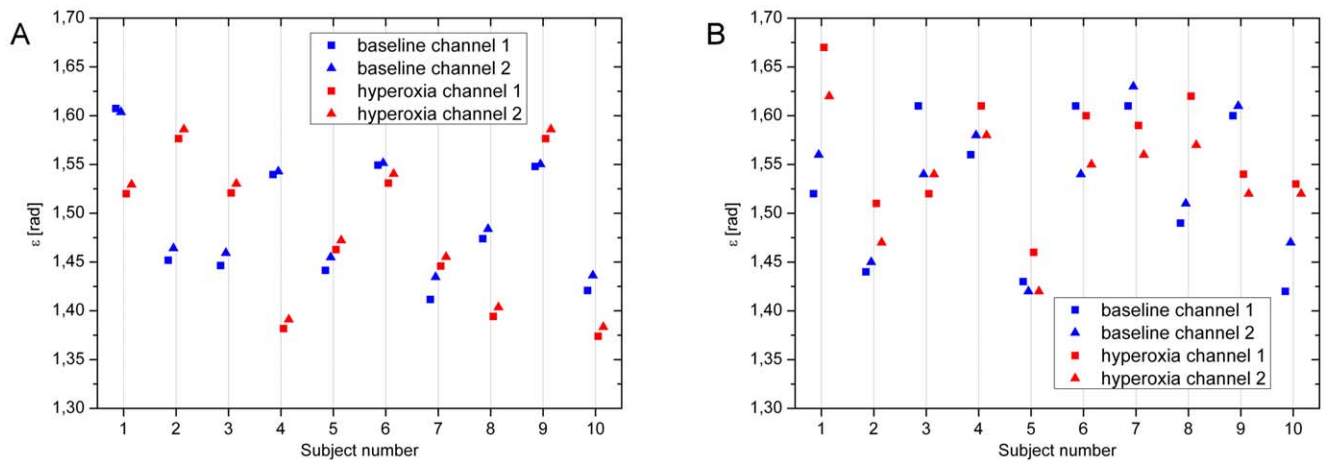doi:10.1371/journal.pone.0045876.g008

theoretical considerations but also from our measurements as presented in Figures 9 and 10. One might argue that for the quantification of relative changes in blood flow, as induced for instance during hyperoxia, no bidirectional system is required. Our data, however, indicate that this is not the case. As can be seen from our angle calculations presented in Figure 10, the angle of incidence changed in all subjects between baseline measurements and measurements during 100% oxygen breathing. One may assume that the problem of sensitivity to changes in the Doppler angle may get less severe with fast acquisition times as achieved for instance with swept source OCT [49]. This is in principle true, but it needs to be considered that blood velocity

even in veins shows pulsatility over the cardiac cycle requiring continuous measurement over several heart cycles in order to get a stable value.

The good agreement between the values of the angle ε as calculated from the two channels of our bidirectional Doppler OCT system also indicates the validity of our model for the extraction of the absolute blood flow velocity. With LDV, the agreement in the calculations is less good. Here, one needs to consider that the bidirectionality of the system is achieved in the detection rather than the illumination pathway. These results most likely reflect the problems in extracting the maximum frequency of the LDV power spectrum as described above.

Figure 9. Sample phase extraction of a baseline measurement. Over the measurement period of 12 s several small eye movements can be seen resulting in pronounced changes in Φ_1 and Φ_2, but almost unchanged $\Delta\Phi$. In addition, the eye also shows a slight overall movement resulting in shifts of Φ_1 and Φ_2 over time.
doi:10.1371/journal.pone.0045876.g009

Figure 10. Calculation of angle ε. Angle ε as calculated from measurements using OCT (red) and LDV (blue) from the two channels. Calculations were done at baseline conditions as well as during hyperoxia.
doi:10.1371/journal.pone.0045876.g010

With the bidirectional LDV system as used in the present study, the maximum velocity that can be measured is determined by the readout rate of the cameras. At higher velocities, phase wrapping prevents adequate data extraction. This problem can be overcome by using faster cameras [22,31], by using resonant Doppler OCT [50] or by using swept source OCT [49]. Other approaches were realized using Doppler OCT with the primary aim to visualize the retinal and choroidal microvasculature [30,51,52,53].

The applications of bidirectional Doppler FD-OCT may be wide. In glaucoma there is a wide body of evidence that perfusion abnormalities are involved in the disease process [3,54,55]. A final proof of this concept is, however, lacking because up to now no technique for the measurement of retinal blood flow was available that could be employed in large-scale population-based studies. Another disease in which Doppler OCT may be of interest is diabetic retinopathy [56]. An early process in diabetic retinopathy is the partial loss of neurovascular coupling [57,58,59,60,61]. This may well contribute to neuronal loss in the diabetic retina, because of oxygen and glucose deprivation during neuronal activity. This concept has been elaborated in some details for the brain [62], but is relatively new for the retina [63,64]. Preliminary data showing

the effect of flicker light stimulation on retinal blood flow using Doppler OCT has been presented recently [65].

In conclusion, the data of the present study indicate that bidirectional Doppler FD-OCT is a valid technique for measuring retinal blood flow velocities. The technique is capable of measuring absolute blood flow velocities, but also to quantify the effect of changes in perfusion such as introduced by 100% oxygen breathing. The Doppler angle is very critical, because only small changes in this angle lead to pronounced changes in the extracted phase. Our in vivo measurements do, however, indicate that the bidirectional approach can be used to overcome this problem. The applications of this technique may be wide including studies in glaucoma and diabetic retinopathy.

Author Contributions

Conceived and designed the experiments: RMW RAL MG GG LS. Performed the experiments: RMW SP RT. Analyzed the data: RMW SP RT RAL GG LS. Contributed reagents/materials/analysis tools: MG LS. Wrote the paper: RMW LS.

References

1. Mozaffarieh M, Flammer J (2007) Is there more to glaucoma treatment than lowering IOP? Surv Ophthalmol 52 Suppl 2: S174–179.
2. Pemp B, Schmetterer L (2008) Ocular blood flow in diabetes and age-related macular degeneration. Can J Ophthalmol 43: 295–301.
3. Schmidl D, Garhofer G, Schmetterer L (2011) The complex interaction between ocular perfusion pressure and ocular blood flow – relevance for glaucoma. Exp Eye Res 93: 141–155.
4. Stalmans I, Vandewalle E, Anderson DR, Costa VP, Frenkel RE, et al. (2011) Use of colour Doppler imaging in ocular blood flow research. Acta Ophthalmol 89: e609–630.
5. Sugiyama T, Araie M, Riva CE, Schmetterer L, Orgul S (2010) Use of laser speckle flowgraphy in ocular blood flow research. Acta Ophthalmol 88: 723–729.
6. Riva CE, Geiser M, Petrig BL (2010) Ocular blood flow assessment using continuous laser Doppler flowmetry. Acta Ophthalmol 88: 622–629.
7. Garhofer G, Bek T, Boehm AG, Gherghel D, Grunwald J, et al. (2010) Use of the retinal vessel analyzer in ocular blood flow research. Acta Ophthalmol 88: 717–722.
8. Riva C, Ross B, Benedek GB (1972) Laser Doppler measurements of blood flow in capillary tubes and retinal arteries. Invest Ophthalmol 11: 936–944.
9. Riva CE, Grunwald JE, Sinclair SH, O'Keefe K (1981) Fundus camera based retinal LDV. Appl Opt 20: 117–120.
10. Riva CE, Grunwald JE, Sinclair SH, Petrig BL (1985) Blood velocity and volumetric flow rate in human retinal vessels. Invest Ophthalmol Vis Sci 26: 1124–1132.
11. Feke GT, Tagawa H, Deupree DM, Goger DG, Sebag J, et al. (1989) Blood flow in the normal human retina. Invest Ophthalmol Vis Sci 30: 58–65.
12. Garhofer G, Werkmeister R, Dragostinoff N, Schmetterer L (2012) Retinal blood flow in healthy young subjects. Invest Ophthalmol Vis Sci 53: 698–703.
13. Yazdanfar S, Rollins AM, Izatt JA (2003) In vivo imaging of human retinal flow dynamics by color Doppler optical coherence tomography. Arch Ophthalmol 121: 235–239.
14. Chen Z, Milner TE, Srinivas S, Wang X, Malekafzali A, et al. (1997) Noninvasive imaging of in vivo blood flow velocity using optical Doppler tomography. Opt Lett 22: 1119–1121.
15. Logean E, Schmetterer LF, Riva CE (2000) Optical Doppler velocimetry at various retinal vessel depths by variation of the source coherence length. Appl Opt 39: 2858–2862.
16. Leitgeb R, Schmetterer L, Drexler W, Fercher A, Zawadzki R, et al. (2003) Real-time assessment of retinal blood flow with ultrafast acquisition by color Doppler Fourier domain optical coherence tomography. Opt Express 11: 3116–3121.
17. Leitgeb RA, Schmetterer L, Hitzenberger CK, Fercher AF, Berisha F, et al. (2004) Real-time measurement of in vitro flow by Fourier-domain color Doppler optical coherence tomography. Opt Lett 29: 171–173.
18. Pedersen CJ, Huang D, Shure MA, Rollins AM (2007) Measurement of absolute flow velocity vector using dual-angle, delay-encoded Doppler optical coherence tomography. Opt Lett 32: 506–508.

19. Iftimia NV, Hammer DX, Ferguson RD, Mujat M, Vu D, et al. (2008) Dual-beam Fourier domain optical Doppler tomography of zebrafish. Opt Express 16: 13624–13636.

20. Wang Y, Lu A, Gil-Flamer J, Tan O, Izatt JA, et al. (2009) Measurement of total blood flow in the normal human retina using Doppler Fourier-domain optical coherence tomography. Br J Ophthalmol 93: 634–637.

21. Wang Y, Fawzi AA, Varma R, Sadun AA, Zhang X, et al. (2011) Pilot study of optical coherence tomography measurement of retinal blood flow in retinal and optic nerve diseases. Invest Ophthalmol Vis Sci 52: 840–845.

22. Singh AS, Kolbitsch C, Schmoll T, Leitgeb RA (2010) Stable absolute flow estimation with Doppler OCT based on virtual circumpapillary scans. Biomed Opt Express 1: 1047–1058.

23. Michaely R, Bachmann AH, Villiger ML, Blatter C, Lasser T, et al. (2007) Vectorial reconstruction of retinal blood flow in three dimensions measured with high resolution resonant Doppler Fourier domain optical coherence tomography. J Biomed Opt 12: 041213.

24. Werkmeister RM, Dragostinoff N, Pircher M, Gotzinger E, Hitzenberger CK, et al. (2008) Bidirectional Doppler Fourier-domain optical coherence tomography for measurement of absolute flow velocities in human retinal vessels. Opt Lett 33: 2967–2969.

25. Kiss B, Polska E, Dorner G, Polak K, Findl O, et al. (2002) Retinal blood flow during hyperoxia in humans revisited: concerted results using different measurement techniques. Microvasc Res 64: 75–85.

26. Tuchin VV (2005) Optical Clearing of Tissue and Blood: SPIE Publications.

27. Gullstrand A (1924) The dioptrics of the eye. In: Southall J, editor. Helmholtz's Treatise on Physiological Optics: Optical Society of America 351–352.

28. Singh AS, Schmoll T, Leitgeb RA (2011) Segmentation of Doppler optical coherence tomography signatures using a support-vector machine. Biomed Opt Express 2: 1328–1339.

29. American National Standards Institute American National Standard for Safe Use of Lasers. Orlando, Fl: The Laser Institute of America; 2000. ANSI Z136.1–22000,.

30. Makita S, Hong Y, Yamanari M, Yatagai T, Yasuno Y (2006) Optical coherence angiography. Opt Express 14: 7821–7840.

31. Schmoll T, Kolbitsch C, Leitgeb RA (2009) Ultra-high-speed volumetric tomography of human retinal blood flow. Opt Express 17: 4166–4176.

32. Zhong Z, Song H, Chui TY, Petrig BL, Burns SA (2011) Noninvasive measurements and analysis of blood velocity profiles in human retinal vessels. Invest Ophthalmol Vis Sci 52: 4151–4157.

33. Szkulmowska A, Szkulmowski M, Kowalczyk A, Wojtkowski M (2008) Phase-resolved Doppler optical coherence tomography – limitations and improvements. Opt Lett 33: 1425–1427.

34. Polak K, Dorner G, Kiss B, Polska E, Findl O, et al. (2000) Evaluation of the Zeiss retinal vessel analyser. Br J Ophthalmol 84: 1285–1290.

35. Pemp B, Polska E, Karl K, Lasta M, Minichmayr A, et al. (2010) Effects of antioxidants (AREDS medication) on ocular blood flow and endothelial function in an endotoxin-induced model of oxidative stress in humans. Invest Ophthalmol Vis Sci 51: 2–6.

36. Garcia JP, Jr., Garcia PT, Rosen RB (2002) Retinal blood flow in the normal human eye using the canon laser blood flowmeter. Ophthalmic Res 34: 295–299.

37. Polska E, Kircher K, Ehrlich P, Vecsei PV, Schmetterer L (2001) RI in central retinal artery as assessed by CDI does not correspond to retinal vascular resistance. Am J Physiol Heart Circ Physiol 280: H1442–1447.

38. Grunwald JE, DuPont J, Riva CE (1996) Retinal haemodynamics in patients with early diabetes mellitus. Br J Ophthalmol 80: 327–331.

39. Grunwald JE, Riva CE, Baine J, Brucker AJ (1992) Total retinal volumetric blood flow rate in diabetic patients with poor glycemic control. Invest Ophthalmol Vis Sci 33: 356–363.

40. Logean E, Schmetterer L, Riva CE (2003) Velocity profile of red blood cells in human retinal vessels using confocal scanning laser Doppler velocimetry. Laser Physics 13: 45–51.

41. Pemp B, Polska E, Garhofer G, Bayerle-Eder M, Kautzky-Willer A, et al. (2010) Retinal blood flow in type 1 diabetic patients with no or mild diabetic retinopathy during euglycemic clamp. Diabetes Care 33: 2038–2042.

42. Feke GT, Buzney SM, Ogasawara H, Fujio N, Goger DG, et al. (1994) Retinal circulatory abnormalities in type 1 diabetes. Invest Ophthalmol Vis Sci 35: 2968–2975.

43. Yoshida A, Feke GT, Mori F, Nagaoka T, Fujio N, et al. (2003) Reproducibility and clinical application of a newly developed stabilized retinal laser Doppler instrument. Am J Ophthalmol 135: 356–361.

44. Nagaoka T (2006) [Physiological mechanism for the regulation of ocular circulation]. Nihon Ganka Gakkai Zasshi 110: 872–878.

45. Riva CE, Grunwald JE, Sinclair SH (1983) Laser Doppler Velocimetry study of the effect of pure oxygen breathing on retinal blood flow. Invest Ophthalmol Vis Sci 24: 47–51.

46. Gilmore ED, Hudson C, Nrusimhadevara RK, Harvey PT, Mandelcorn M, et al. (2007) Retinal arteriolar diameter, blood velocity, and blood flow response to an isocapnic hyperoxic provocation in early sight-threatening diabetic retinopathy. Invest Ophthalmol Vis Sci 48: 1744–1750.

47. Bower BA, Zhao M, Zawadzki RJ, Izatt JA (2007) Real-time spectral domain Doppler optical coherence tomography and investigation of human retinal vessel autoregulation. J Biomed Opt 12: 041214.

48. Linsenmeier RA, Braun RD (1992) Oxygen distribution and consumption in the cat retina during normoxia and hypoxemia. J Gen Physiol 99: 177–197.

49. Baumann B, Potsaid B, Kraus MF, Liu JJ, Huang D, et al. (2011) Total retinal blood flow measurement with ultrahigh speed swept source/Fourier domain OCT. Biomed Opt Express 2: 1539–1552.

50. Bachmann AH, Villiger ML, Blatter C, Lasser T, Leitgeb RA (2007) Resonant Doppler flow imaging and optical vivisection of retinal blood vessels. Opt Express 15: 408–422.

51. Zotter S, Pircher M, Torzicky T, Bonesi M, Gotzinger E, et al. (2011) Visualization of microvasculature by dual-beam phase-resolved Doppler optical coherence tomography. Opt Express 19: 1217–1227.

52. Tao YK, Kennedy KM, Izatt JA (2009) Velocity-resolved 3D retinal microvessel imaging using single-pass flow imaging spectral domain optical coherence tomography. Opt Express 17: 4177–4188.

53. Schmoll T, Singh AS, Blatter C, Schriefl S, Ahlers C, et al. (2011) Imaging of the parafoveal capillary network and its integrity analysis using fractal dimension. Biomed Opt Express 2: 1159–1168.

54. Resch H, Garhofer G, Fuchsjager-Mayrl G, Hommer A, Schmetterer L (2009) Endothelial dysfunction in glaucoma. Acta Ophthalmol 87: 4–12.

55. Flammer J, Orgul S, Costa VP, Orzalesi N, Krieglstein GK, et al. (2002) The impact of ocular blood flow in glaucoma. Prog Retin Eye Res 21: 359–393.

56. Schmetterer L, Wolzt M (1999) Ocular blood flow and associated functional deviations in diabetic retinopathy. Diabetologia 42: 387–405.

57. Garhofer G, Zawinka C, Resch H, Kothy P, Schmetterer L, et al. (2004) Reduced response of retinal vessel diameters to flicker stimulation in patients with diabetes. Br J Ophthalmol 88: 887–891.

58. Mandecka A, Dawczynski J, Blum M, Muller N, Kloos C, et al. (2007) Influence of flickering light on the retinal vessels in diabetic patients. Diabetes Care 30: 3048–3052.

59. Nguyen TT, Kawasaki R, Wang JJ, Kreis AJ, Shaw J, et al. (2009) Flicker light-induced retinal vasodilation in diabetes and diabetic retinopathy. Diabetes Care 32: 2075–2080.

60. Pemp B, Garhofer G, Weigert G, Karl K, Resch H, et al. (2009) Reduced retinal vessel response to flicker stimulation but not to exogenous nitric oxide in type 1 diabetes. Invest Ophthalmol Vis Sci 50: 4029–4032.

61. Nguyen TT, Kawasaki R, Kreis AJ, Wang JJ, Shaw J, et al. (2009) Correlation of light-flicker-induced retinal vasodilation and retinal vascular caliber measurements in diabetes. Invest Ophthalmol Vis Sci 50: 5609–5613.

62. Attwell D, Buchan AM, Charpak S, Lauritzen M, Macvicar BA, et al. (2010) Glial and neuronal control of brain blood flow. Nature 468: 232–243.

63. Metea MR, Newman EA (2006) Glial cells dilate and constrict blood vessels: a mechanism of neurovascular coupling. J Neurosci 26: 2862–2870.

64. Riva CE, Logean E, Falsini B (2005) Visually evoked hemodynamical response and assessment of neurovascular coupling in the optic nerve and retina. Prog Retin Eye Res 24: 183–215.

65. Wang Y, Fawzi AA, Tan O, Zhang X, Huang D (2011) Flicker-induced changes in retinal blood flow assessed by Doppler optical coherence tomography. Biomed Opt Express 2: 1852–1860.